International Journal of Physical Sciences Vol. 7(9), pp. 1509 - 1515, 23 February, 2012
Available online at http://www.academicjournals.org/IJPS
DOI: 10.5897/IJPS11.1328
ISSN 1992 - 1950 ©2012 Academic Journals

Full Length Research Paper

Structural health monitoring and damage assessment Part II: Application of the damage locating vector (DLV) method to the ASCE benchmark structure experimental data

Burcu Gunes[1] and Oguz Gunes[2]*

[1]Department of Civil Engineering, Atilim University, Ankara, Turkey.
[2]Department of Civil Engineering, Cankaya University, Ankara, Turkey.

Accepted 3 February, 2012

This paper builds on the review of structural health monitoring (SHM) and damage assessment approaches provided in a companion paper by presenting an application of the damage locating vector (DLV) approach to the experimental (Phase II) data obtained from the experimental benchmark structure of the IASC-ASCE task group on SHM, which is a laboratory (scaled) size steel frame. Different damage conditions were simulated in the frame for braced and unbraced configurations, and the DLV technique was used to detect and localize damage. The damage identification results were presented and the successes and limitations of the DLV method in detecting and locating the simulated damages were discussed.

Key words: Structural health monitoring (SHM), damage locating vector (DLV), damages, braced, unbraced.

INTRODUCTION

Structural health monitoring (SHM) is the process of implementing a damage identification strategy for civil infrastructures. Damage identification problem involves detection, localization and assessment of the extent of damage in a structure so that it's remaining life can be predicted and possibly extended. SHM encompasses both local and global methods of damage identification. The local methods include visual inspections and non-destructive evaluation tools, such as acoustic emission, ultrasonic, magnetic particle inspection, radiography and eddy current. All these techniques, however, require apriori localization of the damaged zone and easy access to the portion of the structure under inspection. As an alternative that overcomes these limitations, global vibration based methods have been widely developed over the years (Sohn et al., 2003; Chang et al., 2003; Gunes and Gunes, 2012).

Most of the existing damage identification methods can be classified into two groups: model-based and non-model or feature-based methods. The model-based methods are essentially model updating procedures in which the mathematical model or the physical parameters of a structure is calibrated or updated using vibration measurements from the physical structure (Zimmerman and Kaouk 1992; Fritzen et al., 1998). Analytical sensitivities of response parameters to changes in physical properties are used to update modeling assumptions, physical sizing, elastic moduli, etc. The feature-based approaches detect structural changes by detecting damage features in the measured data without the need for an analytical model of the structure. The main task here is the extraction of damage features sensitive to structural changes, so that damage can be identified from the measured vibration response of civil engineering structures. Natural frequency based metrics, mode shape based metrics, structural damping based metrics, modal strain energy based metrics, flexibility based methods and other matrix perturbation approaches, pattern recognition, neural networks and other statistical approaches, non-linear methods based on advanced time-variant transforms are the most commonly utilized features proposed in the literature for

*Corresponding author. E-mail: ogunes@cankaya.edu.tr.

detecting damage in civil engineering structures. The reader is referred to the companion paper (Gunes and Gunes, 2012) for a critical review of the damage assessment methodologies based on up-to-date research and applications reported in the literature.

The objective of this paper is to present the damage localization application performed on the experimental benchmark structure of the IASC-ASCE task group on SHM using the damage locating vector (DLV) method. The performance of the DLV method, therefore, is investigated under realistic conditions of measurement noise, modelling errors and modal truncation which are inherent complications introduced with experimental data. A brief summary of the method is provided, application details are presented and the results are discussed.

Damage locating vector (DLV) method

The DLV approach was developed to map flexibility changes to spatial localization of damage. The basic features of the technique are described next, a more detailed discussion of the theoretical background, discussion on robustness and other issues as well as application to the ASCE benchmark structure analytical (Phase I) data may be found in the studies of Bernal (2002) and Bernal and Gunes (2004).

The basic idea in the DLV approach is that the vectors that span the null-space of the change in flexibility from the undamaged to the damaged states, when treated as loads on the system, lead to stress fields that are zero over the damaged elements. Depending on the number and location of the sensors, the intersection of the null stress regions identified by the DLVs may or may not contain elements that are not damaged in addition to the damaged ones. Elements that are undamaged, but which cannot be discriminated from the damaged ones by changes in flexibility (for a given set of sensors) are inseparable. The steps of the DLV localization can be summarized as follows:

1. Compute the change in flexibility as;

$$DF = F_U - F_D \tag{1}$$

2. Obtain a singular value decomposition of ***DF***, namely;

$$DF = U \begin{bmatrix} s_1 & 0 \\ 0 & s_2 \end{bmatrix} V^T \tag{2}$$

where s_2 are 'small' singular values. For ideal conditions, the s_2 values are zero and the DLV vectors are simply the columns of ***V*** associated with the null space. For the noisy conditions that prevail in practice, however, the values in s_2 are never equal to zero and a cutoff is needed to select the dimension of the effective null space. The steps to make the determination are presented subsequently; the theoretical support can be found in Bernal (2002) and is omitted here for brevity.

1. Consider a vector in ***V*** say V_j
2. Compute the stresses in an undamaged model of the structure using V_j as loads.
3. Reduce the independent internal stresses in every element to a single value denoted as characterizing stress, σ to discriminate between large and small stresses. The characterizing stress is defined in such a way that the strain energy per unit length (or unit area or volume, in 2-D or 3-D elements, respectively) is proportional to σ^2. For a truss bar, for example, σ can be taken as the absolute value of the bar force, whereas for a planar prismatic beam element for which two end moments (m_i and m_j) exist, σ can be taken as $\sqrt{(m_i^2 + m_j^2 + m_i m_j)}$. The reciprocal of the maximum value of the characterizing stress is denoted as c_j.

4. Compute the *svn* index as:

$$svn_j = \sqrt{\frac{s_j c_j^2}{s_q c_q^2}} \tag{3}$$

where

$$s_q c_q^2 = \max(s_j c_j^2) \quad \text{for } j = 1:m \tag{4}$$

5. The vector V_j can be treated as a DLV if:

$$svn_j \le 0.2 \tag{5}$$

Once the DLV vectors have been identified, the localization proper is carried out as follows:

6. Compute, for each DLV vector, the normalized stress index vector as;

$$nsi_i = \frac{\sigma_i}{\sigma_i\big|_{\max}} \tag{6}$$

7. Compute the vector of weighted stress indices, *WSI,* as:

$$WSI = \frac{\sum_{i=1}^{ndlv} \frac{nsi_i}{\overline{svn_i}}}{ndlv} \tag{7}$$

where

$$\overline{svn} = \max(svn, 0.015) \tag{8}$$

and *ndlv* is the number of DLV vectors.

8. The potentially damaged elements are those having *WSI* <1.

It is worth noting that the DLV method was introduced as a technique that can be used to map the changes in the flexibility matrices F_U and F_D of the undamaged and damaged states, respectively to damage locations. The method summarized herein assumes that the synthesized flexibility matrices at both states are readily available. To obtain these matrices, however, one needs to perform modal identification to extract the modal frequencies and the arbitrarily scaled mode-shapes and then obtain the mass normalized mode shapes to synthesize the flexibility matrix. For completeness, the extraction of the flexibility matrices can be summarized as in the following.

Assuming that small vibration amplitude data have been used to obtain the matrices of a state-space realization, in continuous time, one can write:

$$\dot{x} = Ax + Bu \tag{9a}$$

$$y = Cx + Du \tag{9b}$$

Figure 1. (a) Benchmark structure, (b) beam-column connection and (c) a sample accelerometer.

where *A, B, C, D* are the matrices of realization, *x* is the state vector, *u* is the input and *y* is the measured output. Introducing a change of basis to displacement-velocity (D-V) state, the D-V complex eigenvectors can be computed as;

$$\Phi = \begin{bmatrix} C\psi[\lambda]^{-p} \\ C\psi[\lambda]^{-p+1} \end{bmatrix} \quad (10)$$

where ψ and Λ are the displacement partition of the eigenvectors and eigenvalues of the system matrix *A* and *p*=0, 1, or 2 for displacement, velocity and acceleration sensing, respectively.

Taking a Fourier transform of Equations 9a and b, solving for the state vector from Equation 9a and substituting the result into Equation 9b one gets;

$$y(\omega) = \left[C[Ii\omega - A]^{-1} B + D \right] u(\omega) \quad (11)$$

The Fourier transform of the output vector can be expressed in terms of that which corresponds to the displacement vector, y_D as:

$$y(\omega) = (i\omega)^p y_D(\omega) \quad (12)$$

Since the flexibility (*F*) relates $y_D(\omega)$ to $u(\omega)$ at ω=0, defining Boolean matrices q_1 and q_2 so that (F.q_1) and (u.q_2) are the columns of the flexibility and the rows of the input associated with collocated sensors, respectively, one can write:

$$Fq_1 = -CA^{-(p+1)}Bq_2 \quad (13)$$

In the case of full collocation, that is, when q_1 and q_2 are both identities, Equation 13 gives the flexibility matrix directly. This, however, is a special case of full collocation and in general, one is required to use the information given in Equation 13 to extract the mass normalization constants provided that there is, at least, one collocated input-output coordinate. Further details of the mass normalization procedure can be seen in the study of Gunes (2002). Hence, once the flexibility matrices at both the undamaged and damaged states are synthesized, then one can apply the localization procedure as explained in the foregoing.

IASC-ASCE experimental benchmark structure

The experimental benchmark problem is the 4-story, 2-bay by 2-bay steel-frame scale-model structure as shown in Figure 1. The structure is 2.5 × 2.5 m in plan and is 3.6 m tall. The nine vertical columns are bolted to a steel base frame, and the lower flanges of two of the base beams are encased in concrete, fixing the steel frame to the concrete slab. The members are hot-rolled, grade 300 W steel which are specifically designed for this scale model test structure. The columns are B100 × 9 sections and the floor beams are S75 × 11 sections. In each bay, the bracing system consists of two 12.7 mm (0.5 in) diameter threaded steel rods placed in parallel along the diagonal. One floor slab is placed in each bay per floor: four 1000 kg slabs at each of the first, second and third levels, four 750 kg slabs on the fourth floor. These masses are fixed to the structure using two channel sections to bolt each mass to the steel frame. The mass of each channel section is approximately 9.75 kg for a total of 19.5 kg per mass for two channels. Fifteen accelerometers were placed throughout the frame to measure the responses of the test structure and on the base of the frame; 2 per floor measuring the north-south motion of the structure (along the strong axis), and 1 measuring the east-west motion of the structure (along the weak axis) as shown in Figure 2. A series of ambient and forced excitation, including hammer and shaker tests were conducted on the structure with various damage scenarios as shown in Table 1. The shaker tests consisted of a low amplitude vibration introduced by an electromagnetic shaker installed at the roof level on top of a steel plate, at a 45° angle off the main direction of the frame. The shaker level chosen for the test was

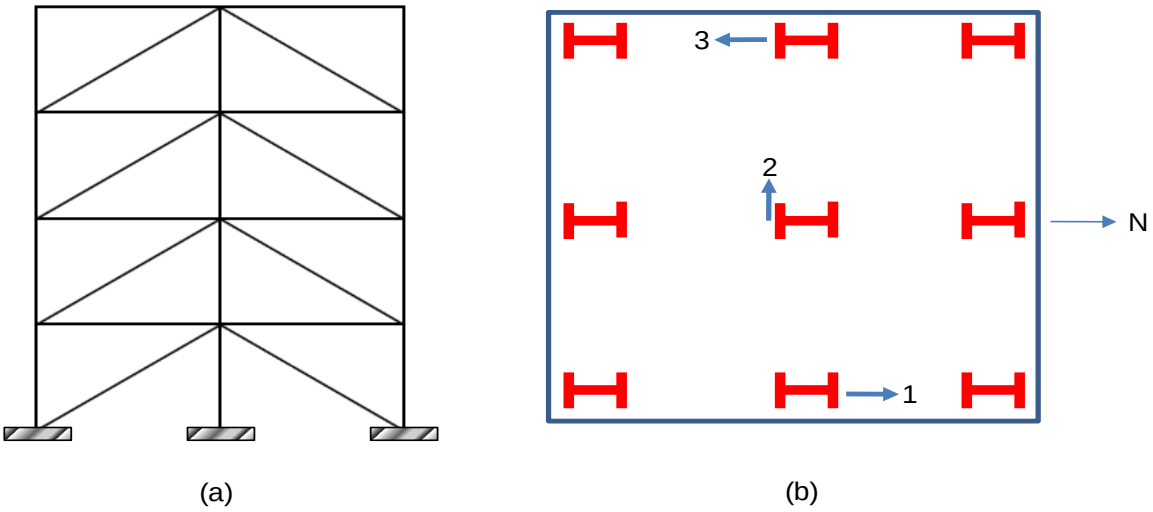

Figure 2. Geometry of the ASCE benchmark structure (a) vertical elevation and (b) floor plan (numbering is for the first floor sensors, the pattern continues in the subsequent floors and 3 sensors per floor).

Table 1. Description of test cases.

Case	Configuration
1	Fully braced configuration
2	All east side braces removed
3	Removed braces on all floors in one bay on southeast corner
4	Removed braces on 1st and 4th floors in one bay on southeast corner
5	Removed braces on 1st floor in one bay on southeast corner
6	Removed braces on all floors on east face, and 2nd floor braces on north face
7	All braces removed on all faces
8	Configuration 7 + loosened bolts on all floors at both ends of beam on east face, north side
9	Configuration 7 + loosened bolts on floors 1 and 2 at both ends of beam on east face, north side

sufficient to produce vibrations larger than those of the ambient vibration tests. In order to capture the induced force to the frame, the acceleration of the shaker was recorded as well. The impact tests were conducted using a Dynatron 5803 A12 Lb Impulse Hammer. The location of the impacts was at the southeast corner of the first level of the frame. In the tests, damage is simulated by removing braces in the structure or by loosening the bolts at beam-column connections (Dyke et al., 2004). This study presents the damage localization results obtained using the impact hammer test data.

Estimation of modal parameters

A critical issue encountered with modal identification techniques is the selection of the correct system/model order which is related to the number of degrees-of-freedom (DOF) of the structure. If a model order higher than the one actually present in the data is assumed, computational modes will arise in order to fulfill the specified model order rather than to represent the dynamic system properties. In order to overcome this limitation, the identification is carried out for increasing model orders. The plots called the stabilization/consistency diagrams are generated to track the modal parameters as a function of increasing model order. After all the solutions are combined in this diagram, physical modes can then be separated from the spurious computational modes by looking for poles which appear at nearly identical frequencies for the different model orders considered.

Figure 3 illustrates the stabilization diagrams for the four tests selected. Note that the system order plotted on the y-axis indicates the size of the state matrix *A*, which is equal to twice the number of modes excited. Once the diagram is prepared, the user is left with the task of separating the physical modes from the computational ones and choosing an estimate among several alternatives that best represents a mode. The consistent-mode indicator function (CMI) can be utilized as a measure to select the best out of two alternatives (Pappa, 1994). Using the stabilization diagrams together with the CMI function, the identified modal parameters for the selected tests are as shown in Table 2. Note that both the fully braced test case (Test 1) and unbraced test case (Test 7) are selected to represent the two healthy systems and Tests 4 and 9 represent the damage scenarios for these two structures, respectively. Eigensystem realization algorithm (ERA) was performed by computing several realizations with varying Hankel

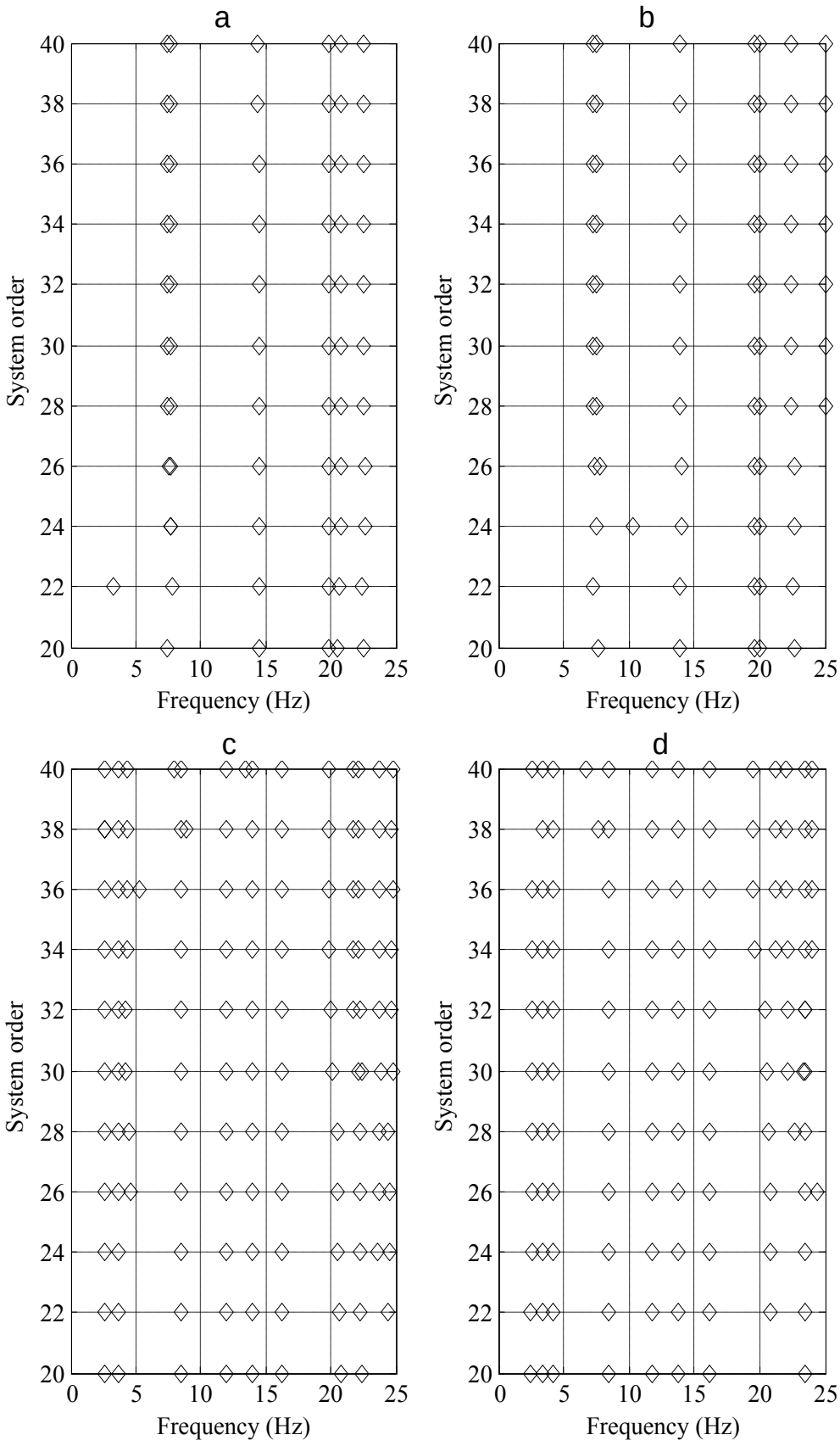

Figure 3. Stability diagrams for the modal frequencies: (a) Test 1, (b) Test 4, (c) Test 7 and (d) Test 9.

Table 2. Modal properties of the braced structure: Healthy and damaged cases.

No.	Braced structure							
	Test 1 (undamaged case)				Test 4 (damaged case)			
	f (Hz)	Zai (%)	CMI (%)	Mode	f (Hz)	Zai (%)	CMI (%)	Mode
1	7.44	0.77	92	TR	7.25	0.85	89	TR
2	7.65	0.64	86	TR	7.56	0.65	97	TR
3	14.45	0.39	88	TO	13.93	0.24	76	TO
4	19.86	0.32	90	TR	19.66	0.36	77	TR
5	20.88	0.42	69	TR	19.93	0.59	80	TR
6	24.74	0.27	89	TR	-	-	-	-

Translation Dominated = TR, Torsion Dominated = TO and Strongly Coupled = SC.

Table 3. Modal properties of the unbraced structure: Healthy and damaged cases.

No.	Unbraced structure							
	Test 7 (undamged case)				Test 9 (damaged case)			
	f (Hz)	ζ (%)	CMI (%)	Mode	f (Hz)	ζ (%)	CMI (%)	Mode
1	2.63	0.36	85	TO	2.57	0.53	98	TO
2	3.60	0.74	84	SC	3.39	0.90	86	SC
3	4.32	0.50	82	TR	4.16	0.36	99	TR
4	8.44	0.36	92	SC	8.38	0.36	100	SC
5	11.93	0.49	98	TR	11.66	0.39	93	TR
6	13.91	0.38	83	SC	13.58T	0.50	91	SC
7	16.15	0.32	91	TR	16.03	0.30	99	TR
8	21.58	0.37	73	TR	20.35	0.81	68	TR
9	23.57	0.66	74	TR	21.05	0.67	69	TR
-	-	-	-	-	23.24	0.74	81	TR

Translation Dominated = TR, Torsion Dominated = TO and Strongly Coupled = SC.

matrix size, forming a stabilization diagram as shown in Figure 3, and selecting the best-extracted modal parameters. The realization leading to a higher complex mode indicator function (CMI) was selected as the correct mode as shown in Tables 2 and 3.

Localization of damage

The previously explained damage locating vector approach was used to localize damage. The weighted stress index (WSI) was computed using a statical model of the structure with a characterizing stress selected based on the type of structure. The potentially damaged elements were identified as those having WSI<=1.0. It should be mentioned that DLVs were computed strictly from the data and the undamaged topology was required to compute the stress fields caused by the DLVs.

A three-dimensional 12-DOF shear building model was used to represent the undamaged state of the structure and the characterizing stress was selected as the story shears and the average of the end moments of the beams for the braced and the unbraced structure, respectively. The associated WSI indices of both cases computed for the frames in north-south and east-west directions are tabulated as shown in Table 4.

RESULTS AND DISCUSSION

As shown in Table 4, although, the approach successfully localized the first and the second floor beams of the frames in the north-south direction as potentially damaged with WSI<1.0, for the unbraced frame; only the fourth floor of the north-south frame has a WSI less than 1 in the braced frame case. The first floor of the north-south frame, with a WSI=4.62, appears to be a ‘false negative’ localization. Approximation in the extraction of the flexibility coefficients as well as the discrepancy between the model used to compute the stress field from the DLVs and the real structure at the healthy state are the two main sources of errors that could lead to this ‘false negative’ identification. The ‘false negative’ results are alerts that should have happened but did not, so in this case, it refers to the case when a truly damaged member is identified as undamaged. From the damage identification point of view, this is an undesirable and a riskier situation than ‘false positives’, because if an undamaged member is identified as potentially damaged, that is not much of a harm, but if a truly damaged member is not detected, the outcome can be disastrous. In this case, however, one could speculate that it is the error in the estimation of the flexibility that has dominated since only one dominantly torsional mode was identified.

Table 4. Weighted stress index for the braced and unbraced frame.

Floor	WSI-braced frame (Case 4) [removed braces on 1st and 4th floors]		WSI-unbraced frame (Case 9) [loosened bolts on floors 1 and 2]	
	North-South	East-West	North-South	East-West
1	4.62	6.73	0.25	4.36
2	7.87	6.92	0.31	4.59
3	5.09	9.68	7.31	5.51
4	0.97	5.71	2.03	3.09

Still, the DLV method provided a 'true' ranking of the elements for the potentially damaged set which can be a very useful feature in prioritization for the screening purposes.

Conclusion

A previous study by Bernal and Gunes (2004) had applied the DLV method to simulated vibration data using the IASC-ASCE benchmark structure model. In this study, the same technique was applied to the experimental vibration data obtained from the real structure for different damage scenarios in braced and unbraced configurations. The method was successful in the identification and localization of damage to a large extent, with the exception of a false negative localization. Further research is currently under-way to improve the accuracy and the robustness of the method for its reliable use in real-life structures.

ACKNOWLEDGEMENTS

The authors would like to thank Professor Dionisio Bernal at Northeastern University for his guidance, collaboration and input in the SHM research by the authors. Appreciation is extended to Professor Shirley Dyke at Purdue University for enabling access to the experimental data and the photos of the ASCE benchmark structure.

REFERENCES

Bernal D (2002). Load vectors for damage localization. J. Eng. Mech., 128(1): 7-14.

Bernal D, Gunes B (2004). A flexibility based approach for the localization and quantification of damage: A benchmark application. J. Eng. Mech., 130: 61-70.

Chang PC, Flatau A, Liu SC (2003). Review paper: Health monitoring of civil infrastructure. Struct. Health Monit., 2(3): 257-267.

Dyke SJ, Bernal D, Beck J, Ventura C (2004). Experimental phase II of the structural health monitoring benchmark problem. 16th Eng. Mech. Conference. University of Washington, Seattle, USA.

Fritzen CP, Jennewein D, Kiefer T (1998). Damage detection based on model updating methods. Mech. Systems Sig. Process., 12(1): 163–86.

Gunes B (2002). Identification and localization of damage: A flexibility based approach. PhD Thesis. Northeastern University, Boston, Massachusetts, USA., p. 163.

Gunes B, Gunes O (2012). Structural Health Monitoring and Damage Assessment Part I: A Critical Review of Approaches and Methods. Int. J. Phys. Sci. (IJPS). İn press.

Pappa R (1994). Eigensystem realization algorithm user's guide for VAX/VMS computers, NASA TM 109066. Langley Research Center, Hampton, Virginia, USA., 571 pp.

Sohn H, Farrar CR, Hemez FM, Shunk DD, Stinemates DW, Nadler BR (2003). A review of structural health monitoring literature: 1996-2001, Los Alamos National Laboratory, USA., 301 pp.

Zimmerman DC, Kaouk M (1992). Eigenstructure assignment approach for structural damage detection. AIAA J., 30(12): 55-1848.